Check for updates

DOI: 10.1177/2045894020935783

Targeting translational read-through of premature termination mutations in *BMPR2* with PTC124 for pulmonary arterial hypertension

Short title: PTC124 improves nonsense BMPR2 mutation expression and function

Lu Long[1*], XuDong Yang[1*], Mark Southwood[2], Stephen Moore[1], Alexi Crosby[1], Paul Upton[1], Benjamin J. Dunmore[1*#], Nicholas W. Morrell[1#]

[*]These authors contributed equally to this work
[#]Joint senior authors

[1]Department of Medicine, University of Cambridge School of Clinical Medicine, Addenbrooke's and Royal Papworth Hospitals, Cambridge, UK
[2]Pathology Research, Royal Papworth Hospital NHS Foundation Trust, Cambridge, UK.

Total Manuscript Pages - 22
Total Figures – 6 (plus 7 supplementary figures)
Words – 5121 (excluding Title Page, Abstract, References and Figure Legends)
Original Research Article

Keywords – Pulmonary Endothelium; Mutations; Translational Research

Confilicting Interests: No conflicts of interest.
Author Contributions: L.L. designed, performed and analysed the majority of the in vitro and in vivo experiments. X.D.Y. performed the majority of the in vitro and in vivo experiments. M.S. performed and analysed histology. S.M. performed and analysed in vivo experiments. A.C. performed and analysed in vivo experiments. P.D.U. contributed to the conception of the study and the design of some experiments. B.J.D. performed in vitro experiments and analysed the majority of the in vitro and in vivo experiments, and wrote the manuscript. N.W.M. conceived the study and the design of multiple experiments, and wrote the manuscript.
Funding: B.J.D., X.D.Y, S.M., A.C., P.D.U. were funded by the British Heart Foundation. This work was funded by awards to N.W.M. (British Heart Foundation Program Grant (RG/13/4/30107) and the Fondation Leducq). Infrastructure support was provided by the Cambridge National Institute for Health Research Biomedical Research Center.

Human Study Ethics - 07/H0306/134 (Cambridgeshire 3 Research Ethics Committee)
Animal Study Ethics - 80/2460 (Home Office Project License)

Address for correspondence:
Professor Nicholas W. Morrell
Division of Respiratory Medicine
Department of Medicine
Box 157, Addenbrooke's Hospital
Hills Road
Cambridge CB2 2QQ
United Kingdom
Tel: +44 1223 331666
Fax : +44 1223 336846
e-mail: nwm23@cam.ac.uk

DOI: 10.1177/2045894020935783

ABSTRACT

Pulmonary arterial hypertension (PAH) is a fatal disorder of the lung circulation in which accumulation of vascular cells progressively obliterates the pulmonary arterioles. This results in sustained elevation in pulmonary artery pressure leading eventually to right heart failure. Approximately, 70% of familial and 20% of sporadic idiopathic PAH cases are caused by mutations in the bone morphogenetic protein receptor type 2 (BMPR2). Nonsense mutations in *BMPR2* are amongst the most common mutations found, where the insertion of a premature termination codon (PTC) causes mRNA degradation via activation of the nonsense-mediated decay (NMD) pathway leading to a state of haploinsufficiency. Ataluren (PTC124), a compound that permits ribosomal read-through of premature stop codons, has been previously reported to increase BMPR2 protein expression in cells derived from PAH patients harbouring nonsense mutations. In this study, we characterized the effects of PTC124 on a range of nonsense *BMPR2* mutations, focusing on the R584X mutation both *in vitro* and *in vivo*. Treatment with PTC124 partially restored BMPR2 protein expression in blood outgrowth endothelial cells (BOECs) isolated from a patient harbouring the R584X mutation. Furthermore, a downstream BMP signalling target, Id1, was rescued by PTC124 treatment. Mutant cells also exhibited increased LPS-induced permeability which was reversed by PTC124 treatment. Increased proliferation and apoptosis in R584C BOECs were also significantly reduced by PTC124. Moreover, oral PTC124 increased lung Bmpr2 protein expression in mice harbouring the R584X mutation (*Bmpr2*$^{+/R584X}$). Our findings provide support for future experimental medicine studies of PTC124 in PAH patients with specific nonsense *BMPR2* mutations.

DOI: 10.1177/2045894020935783

INTRODUCTION

Pulmonary arterial hypertension (PAH) is a devastating disorder characterized by excessive fibroblasts, endothelial cells and smooth muscle cells in the lung vasculature. These aberrant cellular processes cause progressive occlusion of the pulmonary arterioles leading to a sustained elevation in pulmonary artery pressure and eventually right heart failure. Current therapies slow disease progression while also alleviating symptoms, but the only cure remains lung transplantation. Approximately 80% of families with PAH (FPAH), and 20% of apparently idiopathic PAH (IPAH) cases, are due to autosomal dominant heterozygous germline mutations in the bone morphogenetic protein type 2 receptor (*BMPR2*)[1-4]. BMP signalling regulates many processes related to growth, survival, differentiation, and development. Upon BMP ligand stimulation, the constitutively phosphorylated BMPR2 heterodimerizes with BMP type I receptors at the cell surface. A cascade of downstream signalling occurs through phosphorylation of proteins known as receptor-mediated Smads (R-Smads). R-Smads complex with the common partner Smad, Smad4, and translocate to the nucleus driving expression of target genes including the family of Inhibitors of DNA-binding (Ids 1-4)[5]. We have previously shown that mutations in *BMPR2* cause loss-of-function with a reduction in expression of many downstream signalling targets, and altered growth responses to BMP ligands[6-11].

Nonsense mutations introduce premature stop codons into the sequence of DNA. If the mRNA transcript is expressed and translated this can result in a truncated, potentially non-functional protein. Alternately, the mutant transcript is unstable and is rapidly removed by nonsense mediated mRNA decay (NMD)[12], leading to complete absence of the mutant protein. It is estimated that 12% of known disease-causing mutations in the Human Gene Mutation Database are due to nonsense mutations[13], but the functional impact of the premature stop codon can be difficult to predict. Previous studies proposed that variants close to the 3' end of a transcript might avoid NMD[14]. However, a recent large-scale RNA-seq study suggested that up to 68% of variants predicted to cause NMD actually escape RNA surveillance[15]. Since the discovery of mutations in BMPR2 predisposing individuals to PAH, over 300 distinct mutations have been identified with a significant proportion due to nonsense mutations (approximately 30%)[3, 16, 17].

Aminoglycosides such as gentamicin have been used in proof-of-concept studies to suppress NMD as a way of treating cystic fibrosis (CF) and Duchenne muscular dystrophy (DMD)[18-20]. Indeed, gentamicin has been tested successfully in premature termination codon (PTC) *BMPR2* mutations models[21, 22]. However, the risk of renal and otic toxicities due to the requirement of high

DOI: 10.1177/2045894020935783

doses have precluded the use of gentamicin as a therapeutic in this setting. Ataluren (also known as PTC124) is a small molecule non-aminoglycoside oxodiazole, that promotes the readthrough of premature stop codons. Using a high-throughput discovery screen PTC124 was discovered and tested *in vitro* and *in vivo* as a potentially safer alternative to gentamicin[23, 24]. In clinical trials for both CF and DMD, PTC124 appeared safe and showed some promising efficiacy[24-26]. Given these promising findings Drake et al. investigated the ability of PTC124 to improve BMP signalling and reverse the hyperproliferative phenotype in nonsense mutant *BMPR2* endothelial cells[27].

In this study, we further characterised the potential therapeutic properties of PTC124 on a range of PTCs across the *BMPR2* gene in patient-derived cells, and found major differences in the restoration of BMPR2 protein expression between *BMPR2* mutations. Furthermore, we developed a mouse knock-in model for one of these mutations (R584X), to provide proof-of-concept that this approach might be useful in vivo for specific *BMPR2* nonsense mutations.

MATERIALS AND METHODS

Cell Culture and Treatments. Human blood outgrowth endothelial cells (BOECs) were isolated from peripheral blood of PAH patients and healthy controls as previously described[28-30]. All blood donors provided informed consent in accordance with the human study protocol – 07/H0306/134 (Cambridgeshire 3 Research Ethics Committee). Cells were cultured and expanded in EGM-2 (minus heparin) (Lonza, Slough, UK) with 10% FBS (Thermo Fisher Scientific, Hemel Hempstead, UK). All experiments were performed with passage 5-7 cells. Human or mouse PASMCs were isolated as previously described and cultured in DMEM (Invitrogen) containing 20% (v/v) FBS and A/A (DMEM/20%FBS)[31]. The Royal Papworth Hospital ethical review committee approved the use of the human tissues (Ethics Ref 08-H0304-56+5) and informed consent was obtained from all subjects. Recombinant human BMP9 was purchased from R&D Systems (Oxfordshire, UK). Cells were stimulated with BMP9 (10 ng/mL unless otherwise stated) for 4 or 24 hours. PTC124 was a kind gift from PTC Therapeutics (South Plainfield, New Jersey, USA) and was used at 100 μM overnight in all *in vitro* experiments.

Immunoblotting. Frozen lung tissue was homogenised in lysis buffer (250 mM Tris-HCl, pH 6.8, 4% SDS, 20% v/v glycerol and 1x EDTA-free protease inhibitor cocktail - Roche, West Sussex, UK) and sonicated for approximately 1 minute and then centrifuged for 15 minutes at 15,000 x g. BOECs were lysed in lysis buffer (50 mM Tris-HCl, pH 8, 150 mM NaCl, 1% Igepal, 0.5% sodium deoxycholate, 0.1% SDS and 1x EDTA-free protease inhibitor cocktail). The protein concentration

DOI: 10.1177/2045894020935783

was determined using the Bio-Rad Lowry assay (Bio-Rad Laboratories, Hemel Hempstead, UK), using BSA as the standard. Cell lysates (20-100 µg protein) were separated by SDS-PAGE and proteins were transferred to polyvinylidene fluoride membranes by semidry blotting (GE Healthcare, Buckinghamshire, UK). Membranes were then blocked and probed with rabbit monoclonal antibodies toward Id1 (clone 195-14); Id3 (clone 17-3, both CalBioreagents, San Mateo, CA) or mouse monoclonal antibodies against BMPR2 (clone 18/BMPR- II, BD Transduction Laboratories, Wokingham, Berkshire, UK). After washing, blots were incubated with secondary anti-mouse/rabbit horseradish peroxidase antibody (Dako, Cambridgeshire, UK) for 1 hour at room temperature. As a loading control, all blots were re-probed with a monoclonal antibody for either α-tubulin (clone DM1A, Sigma-Aldrich) or β-actin (clone AC-15, Sigma-Aldrich). Densitometry was performed using ImageJ software. Membranes were developed using enhanced chemiluminescence (GE Healthcare).

Endothelial monolayer permeability. Monolayer permeability was assessed as described previously[32]. Briefly, transwell inserts (Corning, Corning, NY) were coated for 1 hour at 37 °C with 0.1 mg/ml bovine skin collagen (Sigma), washed twice with water and rinsed with medium before plating cells. BOECs (400,000 cells in 100 µl Complete EGM-2 medium) were plated in the top chamber and 700 µl of medium was added to the bottom chamber 24 hours before addition of fresh medium to both chambers, with or without 10 ng/ml BMP9 or PTC124 (100 µM) in the upper chamber. After 30 minutes, 25 nM horseradish peroxidase was added to the top chamber, with or without 0.4 µg/ml LPS (Sigma). Medium (20 µl) was collected from the lower chamber every 15 min for 60 min. The horseradish peroxidase content of this medium was determined by measuring absorbance at 490 nm after the addition of 150 µl of *o*-phenylenediamine dihydrochloride buffer to each well of a 96-well plate.

Cell proliferation. For assessment of BOEC proliferation, cells were seeded at 40,000 cells/well in 24-well plates and left to adhere overnight. After 24 hours, cells were then exposed to the stated treatments in EBM-2 containing 2% FBS and A/A. Treatments were replenished every 48 hours. For assessment of mouse PASMC proliferation, cells were seeded at 30,000 cells/well in 24-well plates and left to adhere overnight. After 24 hours, cells were then exposed with or without PTC124 100µM in complete culture media for 48 hours. At the relevant time points, cells were trypsinised and counted on a haemocytometer using trypan blue exclusion to assess cell viability.

DOI: 10.1177/2045894020935783

Apoptosis. Prior to addition of an apoptotic stimulus, BOECs were transferred into EBM-2 basal media (Lonza) with 2% FBS, 100 U/ml penicillin, 100 mg/ml streptomycin and 0.25 mg/ml amphotericin B, but without any growth factor supplements for 16 hours. During this incubation, cells were maintained with or without PTC124 (100 μM) or BMP9 (5 ng/ml) (R&D Systems) for the indicated period. Following the 16 hours incubation, cells were either left unstimulated or treated for 6 hours with 10 ng/ml TNFα and 20 μg/ml cycloheximide to induce apoptosis. Following the apoptotic stimulus cells were trypsinized and stained with FITC-conjugated annexin V and propidium iodide (PI, BD Biosciences, Wokingham, UK) as per the manufacturer's instructions and assessed by flow cytometry. Apoptotic cells were defined as positive for Annexin-V staining and negative for PI staining.

RNA Preparation and Quantitative RT-PCR. Total RNA was extracted using the RNeasy Mini Kit with DNAse digestion (Qiagen, West Sussex, UK). cDNA was prepared from ~1 μg of RNA using the High Capacity Reverse Transcriptase kit (Applied Biosystems, California, USA), according to the manufacturer's instructions. All qPCR reactions were prepared in MicroAmp® optical 384-well reaction plates (Applied Biosystems) using 50 ng/μl cDNA with SYBR®Green Jumpstart™ Taq Readymix™ (Sigma-Aldrich), ROX reference dye (Invitrogen) and sense and anti-sense primers (all 200 nM). Primers for human: *BMPR2*, *ACTB*; mouse: *Bmpr2*, *Actb*, *B2m* and *Hprt* were all designed using Primer3 (http://primer3.sourceforge.net/). Reactions were amplified on a QuantStudio 6Flex Real-Time PCR system (Applied Biosystems). In human BOECs target gene expression was normalized to ACTB and the difference in the amount of product produced was expressed as a fold change. Relative expression of each target gene was identified using the comparative 2-($\Delta\Delta$Ct) method. In mouse lung target gene expression was normalized to *Actb*, *B2m* and *Hprt* and the difference expression represented as relative expression.

Puromycin incubation and RNA isolation. The following protocol was adapted from Hamid and colleagues[22]. BOECs or PASMCs were cultured in full growth media in 6 cm dishes until confluence and then incubated with or without puromycin (100 μg/ml, Sigma Aldrich) 16 hours prior to harvesting. RNA was harvested using the RNeasy Mini kit (QIAGEN) following the manufacturer's instructions.

Reverse Transcriptase Polymerase Chain Reaction (RT-PCR) of BMPR2. Total RNA (~3 μg) was used as a template for cDNA synthesis. Following the manufacturer's protocol, first-strand

DOI: 10.1177/2045894020935783

cDNA synthesis was performed using SuperScript™First-Strand System (Thermo Fisher Scientific) with an oligo-dT primer. A tenth of the first-strand reaction volume was then used as a template for PCR amplification. RT-PCR primers were as follows: W9X - CTTTGCCCTCCTGATTCTTGG (forward) and CTGCTGCCTCCATCATGTTC (reverse); R213X - GAACATGATGGAGGCAGCAG (forward) and CTCGATGGGAAATTGCAGGT (reverse); R321X - CACCACTCAGTCCACCTCAT (forward) and GCGCACCAGTCTATTTCCAG (reverse); R584X - AGACTGTTGGGACCAGGATG (forward) and CGTGAGTCCTGTGGTGTTTG (reverse); R899X - CAACAAGCTGGCCATGATGA (forward) and TGCAAGGTAAACAGCAGTGC (reverse). RT-PCR amplification was conducted using the Elongase™ Enzyme Mix (Thermo Fisher Scientific). Cycling parameters were as follows: Initialisation step - 30 seconds at 94 °C; amplification step (55 cycles) - 94 °C for 30 seconds, 58 °C for 30 seconds, 68 °C for 3 minutes 30 seconds; extension step – 68 °C for 5 minutes. cDNA products were visualised by agarose gel electrophoresis.

DNA sequencing of RT-PCR products. Prior to sequencing, *BMPR2* RT-PCR products were purified with ExoSAP-IT™ PCR Product Cleanup reagent (Thermo Fisher Scientific) according to the manufacturer's protocol. Sequencing reactions were performed using the BigDye™ Terminator v3.1 Cycle Sequencing kit (Thermo Fisher Scientific) according to the manufacturer's protocol. Samples were then sequenced.

***Bmpr2*$^{+/R584X}$ knock-in mouse model.** For all animal work, group sizes were determined using estimates of variance and minimum detectable differences between the groups that were based on our past experience with rodent models of PAH. Animals were randomized using an assigned animal identification number, allowing investigators performing all cardiopulmonary phenotyping procedures and histological analyses to be blinded to animal genotype and treatment group. All animal work was carried out in accordance with the UK Animals (Scientific Procedures) Act 1986 and approved under Home Office Project License 80/2460.

The *Bmpr2*$^{+/R584X}$ knock-in mouse model was generated by GenOway (Lyon, France). Supplementary Figure 5 depicts an overview of the strategy used to generate the R584X mutant. A targeting vector containing the R584X mutation in exon 12 was generated. Upstream of the 3' short homology arm a *lox-P* flanked neomycin cassette was inserted. PCR screening and Southern blot screening were conducted to detect homologous recombination after electroporation into ES cells. Sequence analysis was then conducted to ascertain presence of

DOI: 10.1177/2045894020935783

the R584X mutation. Recombined ES cell clones were injected into blastocysts. To generate chimeric male carrying the recombined locus blastocysts were implanted in pseudo-pregnant females and allowed to develop to term. Chimerism was assessed based on coat colour. Chrimeric males were then bred with Cre-deleter mice to excise the loxP flanked neomycin cassette. Progeny was assessed by genotype analysis.

PTC124 treatment of *Bmpr2*$^{+/R584X}$ animals. Littermate controls (*Bmpr2*$^{+/+}$; n=12) and R584X knock-in (*Bmpr2*$^{+/R584X}$; n=12) mice were randomised into 2 groups. One group was fed chow supplemented with PTC124 (0.3% PTC124) supplied by PTC Therapeutics (South Plainfield, NJ, USA) for 2 weeks. The other group were fed a standard chow diet for 2 weeks. Mice were anesthetized with isoflurane inhalation and then either assessed haemodynamically or mice were exsanguinated and the lungs were removed for further analysis. Lungs were either fixed *in situ* in the distended state by infusion of 10% buffered formalin into the pulmonary artery (at 25 mmHg pressure) via the trachea and overnight fixation in 4% formalin prior to embedding in paraffin, or immediately frozen in liquid nitrogen for protein isolation.

Where indicated in the relevant results section, catheterisation of the right ventricle was undertaken via cannulation of the right internal jugular vein using a Millar SPR-139 catheter (Millar Instruments, Houston, TX) connected to PowerLab hardware utilising LabChart 8 (ADInstruments, Oxford, UK). Mice were then sacrificed and the hearts and lungs were harvested. Right ventricular hypertrophy (RVH) was assessed by removing the heart and dissecting the right ventricle (RV) free wall from the left ventricle plus septum (LV+S) and weighing separately. The degree of right ventricular hypertrophy was determined from the ratio RV/LV+S.

Assessment of Pulmonary Vascular Remodelling. In order to assess pulmonary arteriolar muscularization, sections of fixed mouse lung tissue (5 µm in thickness) were labelled with monoclonal mouse-anti-smooth muscle α-actin (SMA) (clone 1A4, Dako, Glostrup, Denmark), followed by polyclonal goat anti-mouse HRP. To detect staining the Dako ARK^{TM} kit (Dako) was used in accordance with the manufacturer's instructions. Antibody staining was visualised using 3-3’ diaminobenzidine (DAB)–hydrochloride as substrate-chromogen and counterstained with Carrazzi haematoxylin. Pulmonary arteriolar muscularization was assessed by the identification of alveolar ducts and categorization of the accompanying intra-acinar artery as non-, partially or fully muscularized, by the degree of SMA immunostaining. A minimum of 20 vessels with diameters ranging from 25 to 75 µm were categorized as either fully, partially or non-

DOI: 10.1177/2045894020935783

muscularized. Wall thickness was evaluated by the identification of small arteries (<100 μm) proximal to the terminal epithelial bronchioles. Using ImageJ the diameter and thickness of the artery was measured after immunostaining for SMA. Thickness measurements were taken in four different positions of the artery and a minimum of 10 arteries were assessed in each lung section. Assessment of muscularisation and wall thickness were performed in a blinded fashion by a single researcher, to reduce operator variability, who was not aware of the group allocation of the samples being analysed.

PTC124 measurement in serum. PTC124 concentration in mouse serum was conducted using Liquid Chromatography with Mass Spectometry (LC/MS/MS). Serum was isolated from blood samples collected in EDTA tubes at days 7 and 14 by tail vein bleed. Bloods were centrifuged at 2000 x g for 5 minutes, the serum fraction extracted and stored at -80 °C. Samples were analysed using LC/MS/MS by PTC Therapeutics using a UPLC I-Class System and Xevo TQ-S Spectrometer (Waters Corporation, Milford, MA, USA). Briefly, a standard curve of PTC124 was generated (0.01-5 μg/ml). Samples were diluted with 16% methanol and 1 μg/ml D4-124 in acetonitrile. Samples were placed on an automatic shaker for 5 minutes before centrifugation at 2000 rpm for 2 minutes prior to injecting onto the LC/MS/MS system.

Statistics. All data were analysed using GraphPad Prism. Data are presented as mean +/- S.E.M. Data were analysed by one-way/two-way ANOVA with post-hoc Tukey's HSD analysis or paired two-tailed Student's t- test where indicated. $P<0.05$ was considered significant.

RESULTS

Reduced BMPR2 protein expression in BOECs from patients harbouring nonsense *BMPR2* mutations versus controls

Blood outgrowth endothelial cells (BOECs) were available from 4 patients with nonsense mutations in *BMPR2* (W9X, R213X, R321X and R584X), and one patient with a missense mutation in the kinase domain of *BMPR2* (C347R). A further pulmonary artery smooth muscle cell (PASMC) line was available from a PAH patient with a nonsense *BMPR2* mutation (R899X) (Supplementary Figure 1 and Table 1). BMPR2 protein expression was assessed in BOECs from control subjects and *BMPR2* mutant PAH patients. In all mutation patients BMPR2 protein expression was significantly reduced when compared to BOECs isolated from controls (Figure 1A and B). In addition, *BMPR2* mRNA expression in nonsense BMPR2 mutations was significantly reduced (Figure 1C).

DOI: 10.1177/2045894020935783

NMD contributes to reduced expression of mutant transcripts

The reduced mRNA and protein expression and the absence of truncated BMPR2 protein species is consistent with the mutations giving rise to an unstable mRNA transcript that is susceptible to nonsense-mediated mRNA decay (NMD), leading to a state of haploinsufficiency. To assess the abundance of wild type and mutant mRNA species, heterozygous mutant BOECs from PAH patients were used. The relative abundance of wild type and mutant transcripts was assessed by sequencing of cDNA following RT-PCR. In general, all nonsense mutations gave rise to a greatly reduced level of mutant transcript, as evidenced by very low chromatogram signals (Figure 1D and E; Supplementary Figure 2A). The level of mutant transcript varied between mutations with R584X showing the highest transcript level and W9X the lowest. To demonstrate whether NMD was contributing to the reduced mutant transcript level BOECs were treated with puromycin to suppress NMD. Treatment with puromycin increased transcripts of the mutant alleles for all mutations (Figure 1D and E; Supplementary Figure 2A) except W9X (Supplementary Figure 2C). We also assessed the effect of puromycin treatment in PASMCs harbouring a R899X mutation. The baseline R899X transcript level was also greatly reduced, but increased following treatment with puromycin (Supplementary Figure 2B). In Table 2 the predominant transcript is highlighted in bold and the relative fold-change of the mutant transcript versus the wild-type is detailed, +/- puromycin treatment.

PTC124 treatment improves BMPR2 protein expression and downstream signalling in R584X cells

BOECs harbouring heterozygous R213X, R321X and R584X mutations were treated with PTC124 (100 μM) for 24 hours. BMPR2 protein expression was significantly increased by PTC124 in R584X mutant cells but not in R213X or R321X cells (Figure 2A and B). It is worth noting that PTC124 had no effect upon BMPR2 protein expression in control BOECs (Supplementary Figure 3). Furthermore, PTC124 consistently increased Id1 protein levels as a marker of BMPR2 signalling in R584X mutant BOECs (Figure 2C and D). No effect on Id1 levels was observed in control BOECs (Supplementary Figure 3).

Endothelial dysfunction in the R584X mutant is restored by PTC124 treatment

We next questioned whether PTC124 could restore the functional impact of BMPR2 mutation on endothelial cells. First, we examined the effect of PTC124 on endothelial barrier integrity. Monolayer integrity was determined by measuring the amount of horseradish peroxidase leak into

DOI: 10.1177/2045894020935783

the bottom chamber in transwell experiments. Consistent with the results of our previous studies[11], BMP9 treatment inhibited lipopolysaccharide (LPS) induced monolayer permeability in both wild-type and *BMPR2* mutant cells (Figure 3A and B; Supplementary Figure 4A and B). Furthermore, the *BMPR2* mutant BOECs demonstrated greater permeability in the presence of LPS compared to wild-type cells (Figure 4A and B; Supplementary Figure 4A and B). Treatment with PTC124 had no effect on monolayer integrity after LPS stimulation in wild-type or R321X BOECs (Figure 3A; Supplementary Figure 4A and B). However, in R584X BOECs, PTC124 alone significantly reduced the LPS-induced permeability (Figure 3B).

Since increased endothelial apoptosis is considered a critical response to injury in *BMPR2* mutant endothelial cells, we next examined the effect of PTC124 treatment on apoptosis. As previously reported[11], we observed that BOECs harbouring *BMPR2* mutants demonstrate an increased susceptibility to TNFα-induced apoptosis (Figure 4A; Supplementary Figure 5A). Only BOECs with the R584X mutation showed reduced apoptosis when treated with PTC124 (Figure 4A). TNFα-induced apoptosis in BOECs harbouring the R321X mutation was unaffected by treatment with PTC124 (Supplementary Figure 5A).

Finally, we assessed the hyperproliferation of mutant BOECs and the effect of PTC124 treatment. Our group has previously shown that BOECs with *BMPR2* deficiency are hyperproliferative[9]. Both BOECs harbouring the R321X and R584X mutations exhibited hyperproliferation when compared to wild-type BOECs (Figure 4B; Supplementary Figure 5B). Again, only the R584X mutation was significantly affected by PTC124 treatment with a similar reduction in hyperproliferation compared to BMP9 treatment (Figure 4B). Only BMP9 treatment significantly reduced hyperproliferation in R321X mutant cells (Supplementary Figure 5B).

PTC124 improves BMPR2 protein expression in a R584X mouse model

Given that PTC124 exerted promising effects on endothelial function and BMPR2 protein expression in vitro, we developed a knock-in mouse harbouring a heterozygous R584X mutation (*Bmpr2*$^{+/R584X}$) (Supplementary Figure 6) to test the effects of PTC124 *in vivo*. Similar to the findings in patient-derived BOECs, BMPR2 protein and mRNA was significantly reduced in the *Bmpr2*$^{+/R584X}$ mouse lungs compared to littermate controls (Figure 5A, B and E). Mutant *Bmpr2*$^{+/R584X}$ and littermate controls were fed either standard chow or chow supplemented with 0.3% PTC124 over a two-week period. Treatment with PTC124 significantly increased BMPR2 protein expression in *Bmpr2*$^{+/R584X}$ mouse lungs (Figure 5A and C), with no effect observed in wild-

DOI: 10.1177/2045894020935783

type animals (Figure 5A and D). Furthermore, mRNA levels in either wild-type or R584X mutant animals in the presence of PTC124 remained unaffected (Figure 5F and G).

To confirm that mice provided with PTC124 chow attained plasma levels of PTC consistent with a pharmacological effect[24], blood samples were taken at 7 and 14 days for measurement of PTC124 using mass spectrometry. Both mutant and control animals had similar levels of PTC124 at 7- and 14-days treatment (Figure 5D). PTC124 levels was undetectable in control animals fed standard chow (<0.02 µg/ml).

No differences were identified in either right ventricular systolic pressure (RVSP), right ventricular hypertrophy (RVH) or vascular remodelling at 6 months of age (Supplementary Figure 7A and B). Interestingly, during the breeding of this mouse line we noted that parental heterozygous mating occasionally gave rise to homozygous *Bmpr2*$^{R584X/R584X}$ mice. Given that homozygous *Bmpr2*$^{-/-}$ usually die *in utero*, this further suggests that the R584X mutation may have a lower impact on BMPR2 function than other mutations[33].

PTC124 inhibits hyperproliferation in *Bmpr2*$^{+/R584X}$ PASMCs

One well recognized phenotype of human and mouse *BMPR2* mutant PASMCs is heightened proliferation in serum[34, 35]. Consistent with this, PASMCs derived from *Bmpr2*$^{+/R584X}$ mice exhibited increased cell number in the presence of serum after 6 days in culture (Figure 6). Culture of *Bmpr2*$^{+/R584X}$ PASMCs in the presence of PTC124 effectively attenuated the hyperproliferation, with no impact on the proliferation rate of PASMCs from wild type mice.

DISCUSSION

Nonsense mutations account for approximately 30% of *BMPR2* mutations underlying heritable PAH[16]. We have previously proposed that correcting premature stop codons introduced by these mutations might be an approach to treat patients with PAH who carry these mutations[27]. Ataluren (PTC124) has been used in clinical trials in the treatment of cystic fibrosis and Duchenne muscular dystrophy promoting translational readthrough of truncating mutations in CFTR and dystrophin, respectively[24-26]. Our findings suggest that nonsense mutations in *BMPR2* that lead to the introduction of a premature termination codon trigger robust NMD and do not lead the expression of a truncated BMPR2 protein. In fact, the impact of NMD is such that the mutant BMPR2 transcripts are generally expressed at a very low level. This is of major importance for therapeutic approaches, such as PTC124, that act by enhancing translational read-through of the mRNA. In

DOI: 10.1177/2045894020935783

the absence of BMPR2 mRNA these drugs lack the substrate to initiate ribosomal translation into protein the ribosome. Nevertheless, we identified at least one BMPR2 mutation, R584X, that demonstrated measurable levels of mRNA. In this specific case we were able to show that PTC124 increased the expression of BMPR2 protein and downstream signalling both *in vitro* and *in vivo*.

We have previously established a number of functional assays such as vascular permeability, apoptosis and proliferation to test the effectiveness of BMP9 treatment on endothelial cell function[11]. Using these methods, we assessed the ability of PTC124 to rescue the R584X mutant BOECs. We compared cells harbouring the R584X mutation with BOECs expressing R321X, a BMPR2 mutation that previously showed little or no increase in BMPR2 protein expression following PTC124 treatment. Both cell lines exhibited increased vascular permeability compared to the wild-type controls in the presence of LPS which was abrogated by BMP9 treatment. Only cells expressing R584X mutation responded to PTC124 treatment. Of note, no differences were observed with combined BMP9 and PTC124 treatment. Furthermore, the significant increase in apoptosis in both mutant cell lines was only normalised by PTC124 treatment in the R584X BOECs. Similarly, the hyperproliferation phenotype of both BMPR2 mutants was only corrected by PTC124 in the R584X mutant line. Interestingly, BMP9 attenuated the increased proliferation in both *BMPR2* mutant cells.

Given these findings a knock-in R584X mouse model was established. Unfortunately, a lack of haemodynamic or vascular remodelling phenotype was observed in the model. Our experience with other genetic mouse models such as the C118W knock-in mouse, the R899X knock-in, or *Bmpr2* heterozygous null mouse is that these animals develop mild or no pulmonary hypertension, sometimes age-related, but do exhibit morphological evidence of pulmonary vascular remodeling[11, 34, 36]. Therefore, the lack of a pulmonary hypertension phenotype in the $Bmpr2^{+/R584X}$ mouse model is not unexpected. It was more surprising that the mouse exhibited no evidence of pulmonary vascular remodeling. One explanation is that the deficiency of *Bmpr2* in this mouse is less profound that in other Bmpr2 deficient models. This is supported by the appearance of homozygous $Bmpr2^{R584X/R584X}$ mice in our breeding colony. Nevertheless, the $Bmpr2^{+/R584X}$ mouse proved a useful model to demonstrate proof-of-concept and target engagement in the presence of PTC124. Correction of molecular phenotypes was observed in these animals in the presence of PTC124. Firstly, PTC124 was administered in the diet and serum levels indicated therapeutic levels of the drug at week 1 and 2 post administration in both wild-type and $Bmpr2^{+/R584X}$ mice.

DOI: 10.1177/2045894020935783

Similar to our *in vitro* observations in human BOECs, Bmpr2 protein and mRNA expression was significantly reduced in the mutant animals. Treatment with the PTC124 significantly enhanced Bmpr2 protein expression. Furthermore, PTC124 reduced the hyperproliferation of PASMCs isolated from the R584X mutant mouse model.

It appears that PTC124 may have a limited therapeutic role for PAH patients harbouring nonsense mutations in *BMPR2*. The reasons for this could include the efficiency of NMD triggered by these different mutations. The disease-causing PTC mutations we investigated were localised to four domains of the BMPR2 protein – extracellular, transmembrane, kinase and cytoplasmic tail domain. However, the impact and efficiency of NMD are hard to predict. The most commonly proposed mechanism of NMD is the canonical exon junction complex (EJC) model[37, 38]. Ordinarily, EJC proteins bind at exon-exon junctions until they are stripped from mRNAs by the translating ribosome following nuclear export. However, if a PTC is present 50 nucleotides upstream of the last exon boundary then the EJC remains bound triggering NMD. A proposed exception to this model occurs when PTC transcripts in close proximity to the start codon circumvent NMD by reinitiating translation[39, 40]. Lindeboom and colleagues used matched exome and transcriptome data from over 9000 human tumours to further understand the principles governing NMD[41]. Firstly, in the human tumour data the NMD efficiency correlated with the proximity of the PTC to the start codon and the last exon[41]. Secondly, significant reduction in NMD was observed in PTCs that were found in the extremely long exons. Furthermore, the distance between PTC and the downstream exon junction leads to lower degradation rates[41]. Applying the rules to the PTC mutations we tested in BMPR2 may go some way to deciphering why R584X is more susceptible to treatment with PTC124. All mutations tested were 50 nucleotides upstream of the last exon boundary. Only R584X and R899X are located in an exceptionally long exon (exon 12), and the R584X mutation is furthest away from the normal translational stop codon. Therefore, this could make the R584X mutation more likely to be less efficient at NMD.

Duchenne muscular dystrophy (DMD) is caused by mutations in the dystrophin protein. More than 7,000 mutations are associated with either DMD or Becker muscular dystrophy[42]. As the largest human gene, DMD is susceptible to a high mutation rate, which underlies the large variation of mutations detected in the gene. The majority of DMD patients have deletions or duplications in one or more exons, but a small proportion of patients are due to small insertions or deletions (~20%) with a number due to nonsense mutations inserting a premature stop codon with approximately ~10% of dystrophinopathies due to nonsense mutations[43]. In a phase 2b controlled

DOI: 10.1177/2045894020935783

trial, PTC124 was shown to slow disease progression, in boys ≥5 years with a nonsense mutation dystrophinopathy, using the 6-minute walk distance (6MWD) as the primary endpoint[44]. However, in a subsequent phase 3 randomised, double-blinded trial with PTC124 there was no significant difference between the placebo and treated groups based on 6MWD[45]. However, the authors of this study proposed that clinical significance was reached in a subgroup of patients. The authors concluded that ongoing trials should be conducted to assess the long-term benefits and safety of PTC124.

The efficacy of PTC124 has been assessed in cystic fibrosis (CF). In approximately 5-10% of CF patients, nonsense mutations in the gene encoding the CF transmembrane conductance regulator (CFTR) are causative of disease[46] and exhibit a severe clinical phenotype[47]. A preclinical investigation suggested that PTC124 improved the generation of functional CFTR in an animal model of CF due to a nonsense mutation (G542X)[48]. Also, a short-term proof-of-concept trial in patients with nonsense mutations improved epithelial electrophysiological abnormalities caused by dysfunctional CFTR[25]. An extended 12-week study with PTC124 in 19 patients with at least one CFTR nonsense mutation improved total chloride transport[26]. Furthermore, improved CFTR function was associated with improved pulmonary function and reduced CF-related coughing. However, in 2017 PTC therapeutics abandoned a 48-week a phase 3 clinical trial as the two primary endpoints were un met[49].

Overall the clinical trials for both CF and DMD provided inconclusive evidence for the effectiveness of PTC124 as a therapy. However, every study reported that the drug was well tolerated with few toxic side effects. As discussed above, the rules governing NMD are complex and efficiency depends on the location of the premature termination codon in the gene. As we have shown in this study it is possible that PTC124 could provide benefit to a specific subset of PAH patients where NMD is less efficient. For example, apart from R584X, there are 7 nonsense mutations (Y543X, R597X, Q657X, E661X, E672X, Y708X and Q720X) in exon 12 of *BMPR2* that might be benefited by drugs that enhance translational readthrough[3, 17, 50]. The availability of BOECs derived from patients provides an opportunity to test *in vitro* whether individual *BMPR2* mutations might benefit from PTC124. This approach could be used as biomarker in experimental medicine studies and to select patients for inclusion in clinical trials.

DOI: 10.1177/2045894020935783

REFERENCES

1. International PPHC, Lane KB, Machado RD, et al. Heterozygous germline mutations in BMPR2, encoding a TGF-beta receptor, cause familial primary pulmonary hypertension. *Nat Genet* 2000; 26: 81-84. DOI: 10.1038/79226.
2. Deng Z, Morse JH, Slager SL, et al. Familial primary pulmonary hypertension (gene PPH1) is caused by mutations in the bone morphogenetic protein receptor-II gene. *Am J Hum Genet* 2000; 67: 737-744. DOI: 10.1086/303059.
3. Machado RD, Eickelberg O, Elliott CG, et al. Genetics and genomics of pulmonary arterial hypertension. *J Am Coll Cardiol* 2009; 54: S32-42. DOI: 10.1016/j.jacc.2009.04.015.
4. Evans JD, Girerd B, Montani D, et al. BMPR2 mutations and survival in pulmonary arterial hypertension: an individual participant data meta-analysis. *Lancet Respir Med* 2016; 4: 129-137. DOI: 10.1016/S2213-2600(15)00544-5.
5. Massague J, Seoane J and Wotton D. Smad transcription factors. *Genes Dev* 2005; 19: 2783-2810. DOI: 10.1101/gad.1350705.
6. Jeffery TK, Upton PD, Yang X, et al. Does BMPR2 mutation disrupt pulmonary vasculogenesis? *Chest* 2005; 128: 602S. 2005/12/24. DOI: 10.1378/chest.128.6_suppl.602S.
7. Sobolewski A, Rudarakanchana N, Upton PD, et al. Failure of bone morphogenetic protein receptor trafficking in pulmonary arterial hypertension: potential for rescue. *Hum Mol Genet* 2008; 17: 3180-3190. 2008/07/24. DOI: 10.1093/hmg/ddn214.
8. Affara M, Sanders D, Araki H, et al. Vasohibin-1 is identified as a master-regulator of endothelial cell apoptosis using gene network analysis. *BMC Genomics* 2013; 14: 23. DOI: 10.1186/1471-2164-14-23.
9. Caruso P, Dunmore BJ, Schlosser K, et al. Identification of MicroRNA-124 as a Major Regulator of Enhanced Endothelial Cell Glycolysis in Pulmonary Arterial Hypertension via PTBP1 (Polypyrimidine Tract Binding Protein) and Pyruvate Kinase M2. *Circulation* 2017; 136: 2451-2467. 2017/10/04. DOI: 10.1161/CIRCULATIONAHA.117.028034.
10. Long L, Yang X, Southwood M, et al. Chloroquine prevents progression of experimental pulmonary hypertension via inhibition of autophagy and lysosomal bone morphogenetic protein type II receptor degradation. *Circ Res* 2013; 112: 1159-1170. 2013/03/01. DOI: 10.1161/CIRCRESAHA.111.300483.
11. Long L, Ormiston ML, Yang X, et al. Selective enhancement of endothelial BMPR-II with BMP9 reverses pulmonary arterial hypertension. *Nat Med* 2015; 21: 777-785. 2015/06/16. DOI: 10.1038/nm.3877.
12. Isken O and Maquat LE. Quality control of eukaryotic mRNA: safeguarding cells from abnormal mRNA function. *Genes Dev* 2007; 21: 1833-1856. 2007/08/03. DOI: 10.1101/gad.1566807.
13. Stenson PD, Mort M, Ball EV, et al. The Human Gene Mutation Database: building a comprehensive mutation repository for clinical and molecular genetics, diagnostic testing and personalized genomic medicine. *Hum Genet* 2014; 133: 1-9. 2013/10/01. DOI: 10.1007/s00439-013-1358-4.
14. Nagy E and Maquat LE. A rule for termination-codon position within intron-containing genes: when nonsense affects RNA abundance. *Trends Biochem Sci* 1998; 23: 198-199. 1998/06/30. DOI: 10.1016/s0968-0004(98)01208-0.
15. Lappalainen T, Sammeth M, Friedlander MR, et al. Transcriptome and genome sequencing uncovers functional variation in humans. *Nature* 2013; 501: 506-511. 2013/09/17. DOI: 10.1038/nature12531.
16. Graf S, Haimel M, Bleda M, et al. Identification of rare sequence variation underlying heritable pulmonary arterial hypertension. *Nat Commun* 2018; 9: 1416. 2018/04/14. DOI: 10.1038/s41467-018-03672-4.

17. Machado RD, Southgate L, Eichstaedt CA, et al. Pulmonary Arterial Hypertension: A Current Perspective on Established and Emerging Molecular Genetic Defects. *Hum Mutat* 2015; 36: 1113-1127. 2015/09/22. DOI: 10.1002/humu.22904.
18. Politano L, Nigro G, Nigro V, et al. Gentamicin administration in Duchenne patients with premature stop codon. Preliminary results. *Acta Myol* 2003; 22: 15-21. 2003/09/12.
19. Clancy JP, Bebok Z, Ruiz F, et al. Evidence that systemic gentamicin suppresses premature stop mutations in patients with cystic fibrosis. *Am J Respir Crit Care Med* 2001; 163: 1683-1692. 2001/06/13. DOI: 10.1164/ajrccm.163.7.2004001.
20. Wilschanski M, Yahav Y, Yaacov Y, et al. Gentamicin-induced correction of CFTR function in patients with cystic fibrosis and CFTR stop mutations. *N Engl J Med* 2003; 349: 1433-1441. 2003/10/10. DOI: 10.1056/NEJMoa022170.
21. Nasim MT, Ghouri A, Patel B, et al. Stoichiometric imbalance in the receptor complex contributes to dysfunctional BMPR-II mediated signalling in pulmonary arterial hypertension. *Hum Mol Genet* 2008; 17: 1683-1694. 2008/03/07. DOI: 10.1093/hmg/ddn059.
22. Hamid R, Hedges LK, Austin E, et al. Transcripts from a novel BMPR2 termination mutation escape nonsense mediated decay by downstream translation re-initiation: implications for treating pulmonary hypertension. *Clin Genet* 2010; 77: 280-286. 2010/01/26. DOI: 10.1111/j.1399-0004.2009.01311.x.
23. Austin ED, Phillips JA, Cogan JD, et al. Truncating and missense BMPR2 mutations differentially affect the severity of heritable pulmonary arterial hypertension. *Respir Res* 2009; 10: 87. DOI: 10.1186/1465-9921-10-87.
24. Welch EM, Barton ER, Zhuo J, et al. PTC124 targets genetic disorders caused by nonsense mutations. *Nature* 2007; 447: 87-91. 2007/04/24. DOI: 10.1038/nature05756.
25. Kerem E, Hirawat S, Armoni S, et al. Effectiveness of PTC124 treatment of cystic fibrosis caused by nonsense mutations: a prospective phase II trial. *Lancet* 2008; 372: 719-727. 2008/08/30. DOI: 10.1016/S0140-6736(08)61168-X.
26. Wilschanski M, Miller LL, Shoseyov D, et al. Chronic ataluren (PTC124) treatment of nonsense mutation cystic fibrosis. *Eur Respir J* 2011; 38: 59-69. 2011/01/15. DOI: 10.1183/09031936.00120910.
27. Drake KM, Dunmore BJ, McNelly LN, et al. Correction of nonsense BMPR2 and SMAD9 mutations by ataluren in pulmonary arterial hypertension. *Am J Respir Cell Mol Biol* 2013; 49: 403-409. DOI: 10.1165/rcmb.2013-0100OC.
28. Geti I, Ormiston ML, Rouhani F, et al. A practical and efficient cellular substrate for the generation of induced pluripotent stem cells from adults: blood-derived endothelial progenitor cells. *Stem Cells Transl Med* 2012; 1: 855-865. 2013/01/04. DOI: 10.5966/sctm.2012-0093.
29. Ormiston ML, Deng Y, Stewart DJ, et al. Innate immunity in the therapeutic actions of endothelial progenitor cells in pulmonary hypertension. *Am J Respir Cell Mol Biol* 2010; 43: 546-554. 2009/12/10. DOI: 10.1165/rcmb.2009-0152OC.
30. Ormiston ML, Toshner MR, Kiskin FN, et al. Generation and Culture of Blood Outgrowth Endothelial Cells from Human Peripheral Blood. *J Vis Exp* 2015: e53384. 2016/01/19. DOI: 10.3791/53384.
31. Yang X, Long L, Southwood M, et al. Dysfunctional Smad signaling contributes to abnormal smooth muscle cell proliferation in familial pulmonary arterial hypertension. *Circ Res* 2005; 96: 1053-1063. DOI: 10.1161/01.RES.0000166926.54293.68.
32. Harrington EO, Brunelle JL, Shannon CJ, et al. Role of protein kinase C isoforms in rat epididymal microvascular endothelial barrier function. *Am J Respir Cell Mol Biol* 2003; 28: 626-636. 2003/04/23. DOI: 10.1165/rcmb.2002-0085OC.
33. Beppu H, Kawabata M, Hamamoto T, et al. BMP type II receptor is required for gastrulation and early development of mouse embryos. *Dev Biol* 2000; 221: 249-258. 2000/04/25. DOI: 10.1006/dbio.2000.9670.

34. Dunmore BJ, Yang X, Crosby A, et al. 4PBA Restores Signalling of a Cysteine-substituted Mutant BMPR2 Receptor Found in Patients with PAH. *Am J Respir Cell Mol Biol* 2020 2020/04/08. DOI: 10.1165/rcmb.2019-0321OC.
35. Davies RJ, Holmes AM, Deighton J, et al. BMP type II receptor deficiency confers resistance to growth inhibition by TGF-beta in pulmonary artery smooth muscle cells: role of proinflammatory cytokines. *Am J Physiol Lung Cell Mol Physiol* 2012; 302: L604-615. 2012/01/10. DOI: 10.1152/ajplung.00309.2011.
36. Long L, MacLean MR, Jeffery TK, et al. Serotonin increases susceptibility to pulmonary hypertension in BMPR2-deficient mice. *Circ Res* 2006; 98: 818-827. 2006/02/25. DOI: 10.1161/01.RES.0000215809.47923.fd.
37. Zhang J, Sun X, Qian Y, et al. At least one intron is required for the nonsense-mediated decay of triosephosphate isomerase mRNA: a possible link between nuclear splicing and cytoplasmic translation. *Mol Cell Biol* 1998; 18: 5272-5283. 1998/08/26. DOI: 10.1128/mcb.18.9.5272.
38. Thermann R, Neu-Yilik G, Deters A, et al. Binary specification of nonsense codons by splicing and cytoplasmic translation. *EMBO J* 1998; 17: 3484-3494. 1998/06/17. DOI: 10.1093/emboj/17.12.3484.
39. Zhang Z, Lee CH, Mandiyan V, et al. Sequence-specific recognition of the internalization motif of the Alzheimer's amyloid precursor protein by the X11 PTB domain. *EMBO J* 1997; 16: 6141-6150. 1997/10/08. DOI: 10.1093/emboj/16.20.6141.
40. Romao L, Inacio A, Santos S, et al. Nonsense mutations in the human beta-globin gene lead to unexpected levels of cytoplasmic mRNA accumulation. *Blood* 2000; 96: 2895-2901. 2000/10/07.
41. Lindeboom RG, Supek F and Lehner B. The rules and impact of nonsense-mediated mRNA decay in human cancers. *Nat Genet* 2016; 48: 1112-1118. 2016/09/13. DOI: 10.1038/ng.3664.
42. Bladen CL, Salgado D, Monges S, et al. The TREAT-NMD DMD Global Database: analysis of more than 7,000 Duchenne muscular dystrophy mutations. *Hum Mutat* 2015; 36: 395-402. 2015/01/22. DOI: 10.1002/humu.22758.
43. Dent KM, Dunn DM, von Niederhausern AC, et al. Improved molecular diagnosis of dystrophinopathies in an unselected clinical cohort. *Am J Med Genet A* 2005; 134: 295-298. 2005/02/22. DOI: 10.1002/ajmg.a.30617.
44. Bushby K, Finkel R, Wong B, et al. Ataluren treatment of patients with nonsense mutation dystrophinopathy. *Muscle Nerve* 2014; 50: 477-487. 2014/07/22. DOI: 10.1002/mus.24332.
45. McDonald CM, Campbell C, Torricelli RE, et al. Ataluren in patients with nonsense mutation Duchenne muscular dystrophy (ACT DMD): a multicentre, randomised, double-blind, placebo-controlled, phase 3 trial. *Lancet* 2017; 390: 1489-1498. 2017/07/22. DOI: 10.1016/S0140-6736(17)31611-2.
46. Bobadilla JL, Macek M, Jr., Fine JP, et al. Cystic fibrosis: a worldwide analysis of CFTR mutations--correlation with incidence data and application to screening. *Hum Mutat* 2002; 19: 575-606. 2002/05/15. DOI: 10.1002/humu.10041.
47. de Gracia J, Mata F, Alvarez A, et al. Genotype-phenotype correlation for pulmonary function in cystic fibrosis. *Thorax* 2005; 60: 558-563. 2005/07/05. DOI: 10.1136/thx.2004.031153.
48. Du M, Liu X, Welch EM, et al. PTC124 is an orally bioavailable compound that promotes suppression of the human CFTR-G542X nonsense allele in a CF mouse model. *Proc Natl Acad Sci U S A* 2008; 105: 2064-2069. 2008/02/15. DOI: 10.1073/pnas.0711795105.
49. Konstan MW, VanDevanter DR, Rowe SM, et al. Efficacy and safety of ataluren in patients with nonsense-mutation cystic fibrosis not receiving chronic inhaled aminoglycosides:

DOI: 10.1177/2045894020935783

The international, randomized, double-blind, placebo-controlled Ataluren Confirmatory Trial in Cystic Fibrosis (ACT CF). *J Cyst Fibros* 2020 2020/01/28. DOI: 10.1016/j.jcf.2020.01.007.
50. Machado RD, Aldred MA, James V, et al. Mutations of the TGF-beta type II receptor BMPR2 in pulmonary arterial hypertension. *Hum Mutat* 2006; 27: 121-132. 2006/01/24. DOI: 10.1002/humu.20285.

TABLES AND FIGURES

Table 1: Demographics of BMPR2 mutant BOECs

	Gender	Age	Ethinicity	mPAP
W9X	Female	35	Caucasian	65
R213X	Female	36	Asian	40
R321X	Male	45	Caucasian	46
R584X	Female	79	Caucasian	52
R899X	Female	30	N/A	N/A
C347R	Male	27	Caucasian	N/A

Table 2: Puromycin treatment of BMPR2 mutant BOECs. The fold change is calculated by the ratio of the mutant allele peak height/wild-type peak height in the appropriate chromatograms.

	Wild-type allele	Mutant allele	Puromycin -ve	Ratio of M/W (fold change)	Puromycin +ve	Ratio of M/W (fold change)
W9X	TGG	TGA	**TGG**	**0.079**	**TGG**	**0.106**
R213X	CGA	TGA	**CGA**	**0.154**	**CGA**	**0.609**
R321X	CGA	TGA	**CGA**	**0.153**	**CGA**	**0.568**
R584X	CGA	TGA	**CGA**	**0.587**	**TGA**	**1.697**
R899X	CGA	TGA	**CGA**	**0.259**	**CGA**	**0.545**

DOI: 10.1177/2045894020935783

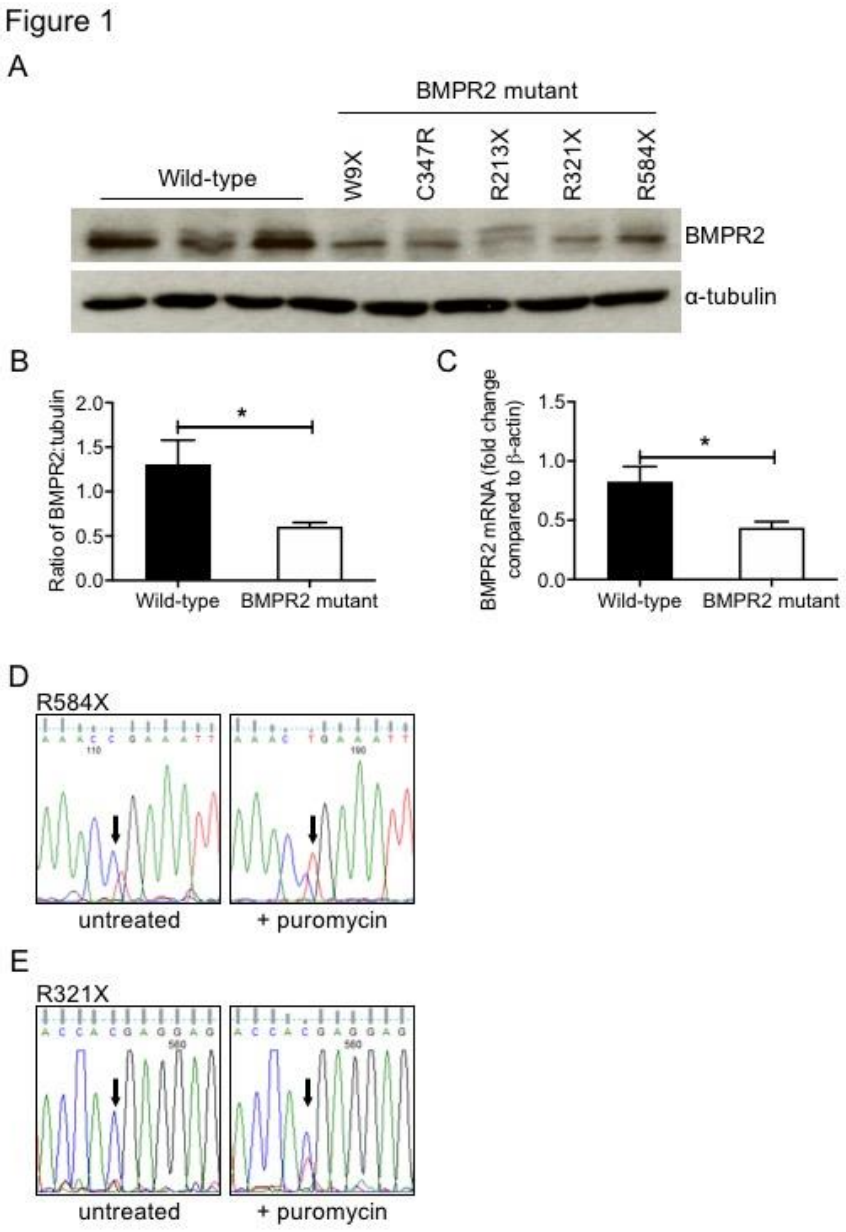

Figure 1. Puromycin treatment increases *BMPR2* R584X mutant transcript. (**A**) Protein lysates were extracted from blood outgrowth endothelial cells (BOECs) from wild-type (n=3) and BMPR2 mutant (n=5) patients. Lysates were immunoblotted for BMPR2 and loading control, α-tubulin. (**B**) Densitometry analysis of the ratio between BMPR2 and α-tubulin. (**C**) *BMPR2* mRNA expression of BOECs harbouring nonsense mutations was assessed and normalised to *ACTB*. (**D** and **E**) BOECs harbouring a R584X or R321X were treated overnight with puromycin (100 mg/ml). Following RNA isolation amplified RT-PCR products were sequenced. Chromatograms for R584X (**D**) and R321X (**E**) show the effects of puromycin treatment on transcript expression. One-way ANOVA. *P≤0.05. Error bars represent mean ± s.e.m.

DOI: 10.1177/2045894020935783

Figure 2

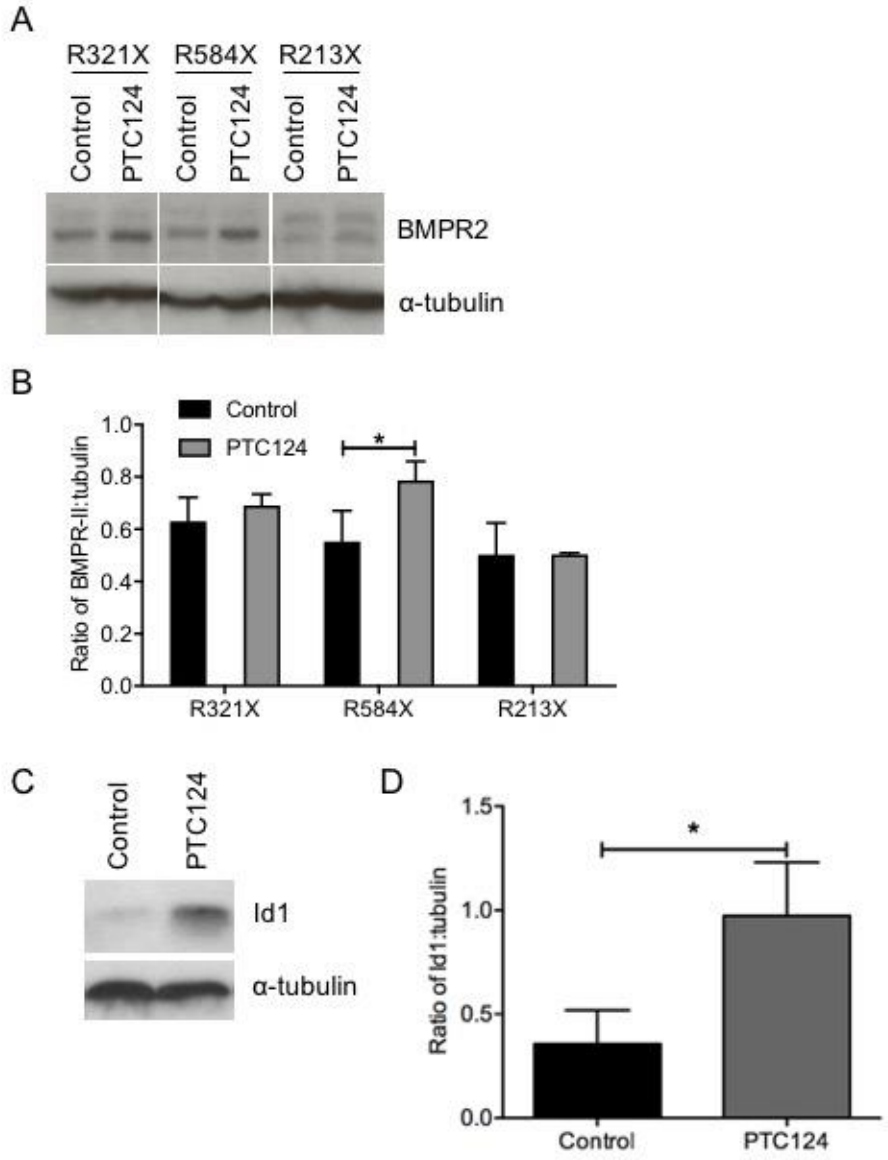

Figure 2. PTC124 treatment increases BMPR2 protein expression and downstream signalling in R584X mutant BOECs (**A**) BOECs isolated from patients habouring R213X, R321X and R584X were treated with either PTC124 (100 μM) for 24 hours. Lysates were immunoblotted for BMPR2 and loading control, α-tubulin (n=3). (**B**) Densitometry analysis of the ratio between BMPR2 and α-tubulin. (**C**) R584X mutant BOECs were treated with PTC124 (100 μM) for 24 hours. Representative immunoblot for Id1 and loading control, α-tubulin (n=3). (**D**) Densitometry analysis of the ratio of α-tubulin compared to Id1 (n=3). Student's t-Test. *P≤0.05. Error bars represent mean ± s.e.m.

DOI: 10.1177/2045894020935783

Figure 3

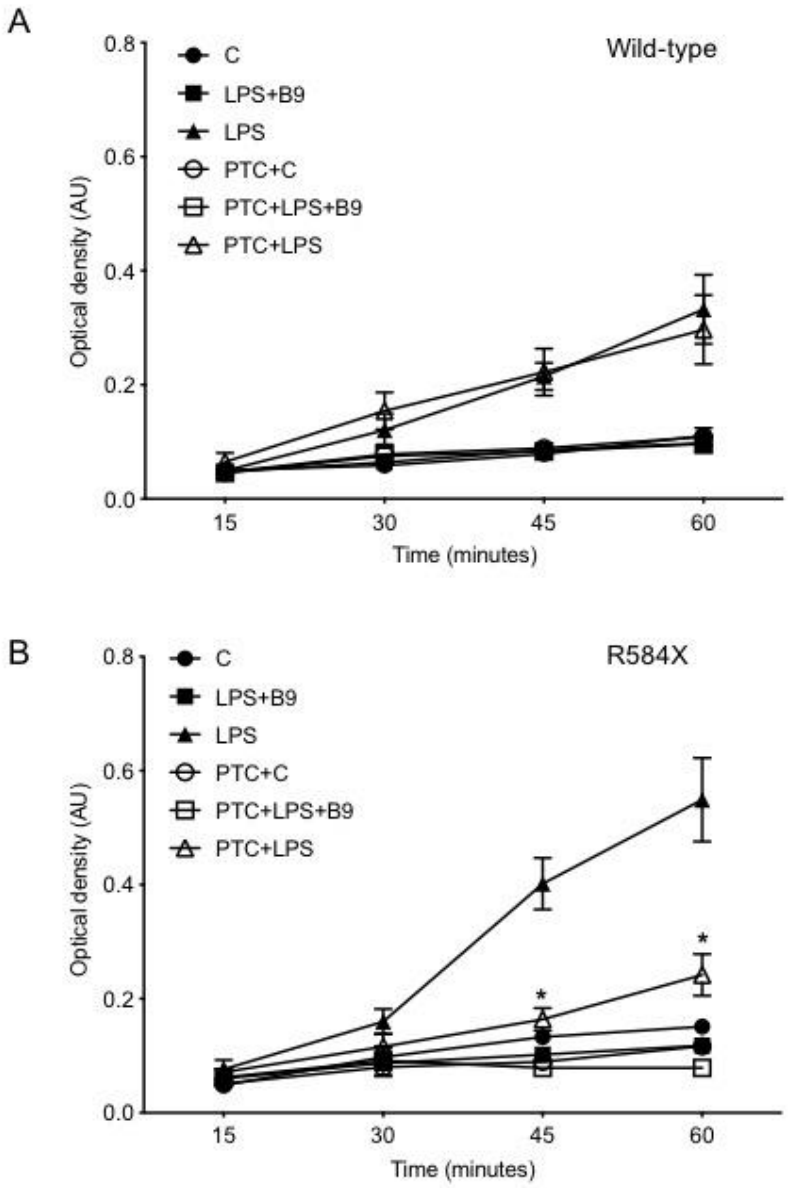

Figure 3. PTC124 treatment promotes monolayer integrity in R584X mutant BOECs. Permeability was assessed in monolayers of wild-type (**A**) (n=3) and R584X mutant (**B**) (n=3) BOECs treated with either PTC124 (100 μM) or BMP9 (0.2 ng/ml) and/or LPS (400 ng/ml). Colorimetric absorbance of HRP was measured after incubation periods every 15 minutes until 1 hour. One-way ANOVA. *P≤0.05. Error bars represent mean ± s.e.m.

DOI: 10.1177/2045894020935783

Figure 4

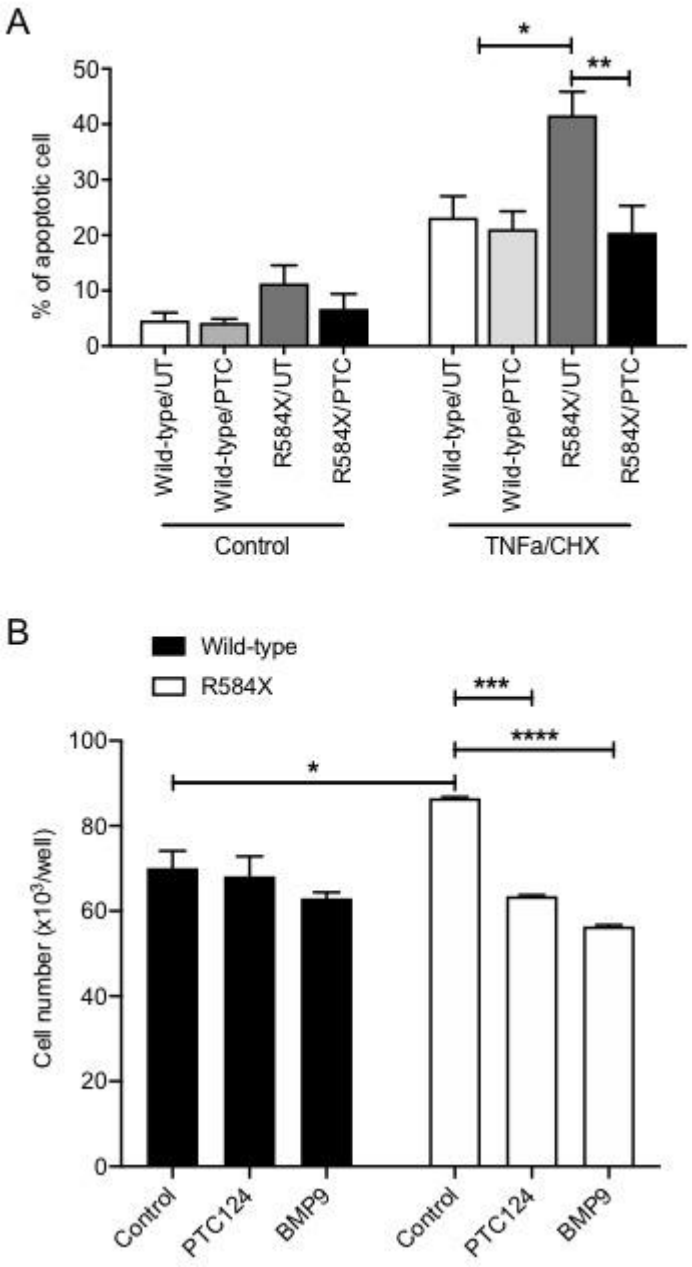

Figure 4. PTC124 treatment prevents apoptosis and hyperproliferation in R584X mutant BOECs. (**A**) Quantification of apoptotic (Annexin-V^+/PI^-) wild-type (n=3) and R584X mutant BOECs (n=3) after PTC124 treatment for 24 hours prior to the addition of TNFa (10 ng/ml) and cycloheximide (20 mg/ml) for 6 hours. (**B**) Proliferation assessment of wild-type (n=3) and R584X mutant (n=3) BOECs after day 6, following PTC124 (100 μM) or BMP9 (5 ng/ml) treatment. One-way ANOVA. *P≤0.05, **P≤0.01, ***P≤0.001, ****P≤0.0001. Error bars represent mean ± s.e.m.

DOI: 10.1177/2045894020935783

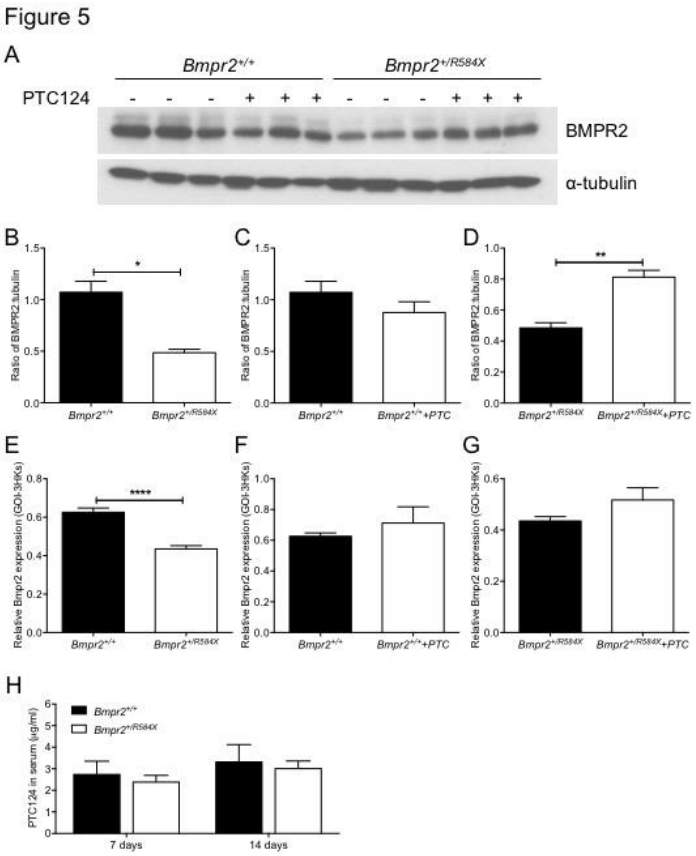

Figure 5. PTC124 treatment rescues low BMPR2 protein expression. Littermate controls (*Bmpr2*$^{+/+}$) and R584X knock-in (*Bmpr2*$^{+/R584X}$) mice were randomised into 2 treatment groups. One group was fed chow supplemented with PTC124 and the other group were fed a standard chow diet for 2 weeks. (**A**) Lungs were isolated from wild-type (*Bmpr2*$^{+/+}$) (n=3); wild-type plus PTC124 (*Bmpr2*$^{+/+}$+PTC124) (n=3); R584X knock-in (*Bmpr2*$^{+/R584X}$) (n=3); R584X knock-in (*Bmpr2*$^{+/R584X}$+PTC124) (n=3). Protein lysates were extracted and immunoblotted for BMPR2 and loading control, α-tubulin (n=3). (**B**) Densitometry analysis of the ratio between BMPR2 and α-tubulin in *Bmpr2*$^{+/+}$ versus *Bmpr2*$^{+/R584X}$. (**C**) Densitometry analysis of the ratio between BMPR2 and α-tubulin in *Bmpr2*$^{+/+}$ versus *Bmpr2*$^{+/+}$+PTC124. (**D**) Densitometry analysis of the ratio between BMPR2 and α-tubulin in *Bmpr2*$^{+/R584X}$ versus *Bmpr2*$^{+/R584X}$+PTC124. (**E**, **F** and **G**) Lungs were isolated from wild-type (*Bmpr2*$^{+/+}$) (n=7); wild-type plus PTC124 (*Bmpr2*$^{+/+}$+PTC124) (n=4); R584X knock-in (*Bmpr2*$^{+/R584X}$) (n=7); R584X knock-in (*Bmpr2*$^{+/R584X}$+PTC124) (n=3). *Bmpr2* mRNA expression was assessed and normalised to 3 endogenous controls (*Actb*, *B2m* and *Hprt*). (**H**) PTC124 levels was measured by MS/LC/LC in the serum of PTC124 treated animals at day 7 and day14. Student's t-Test. *P≤0.05. Error bars represent mean ± s.e.m.

DOI: 10.1177/2045894020935783

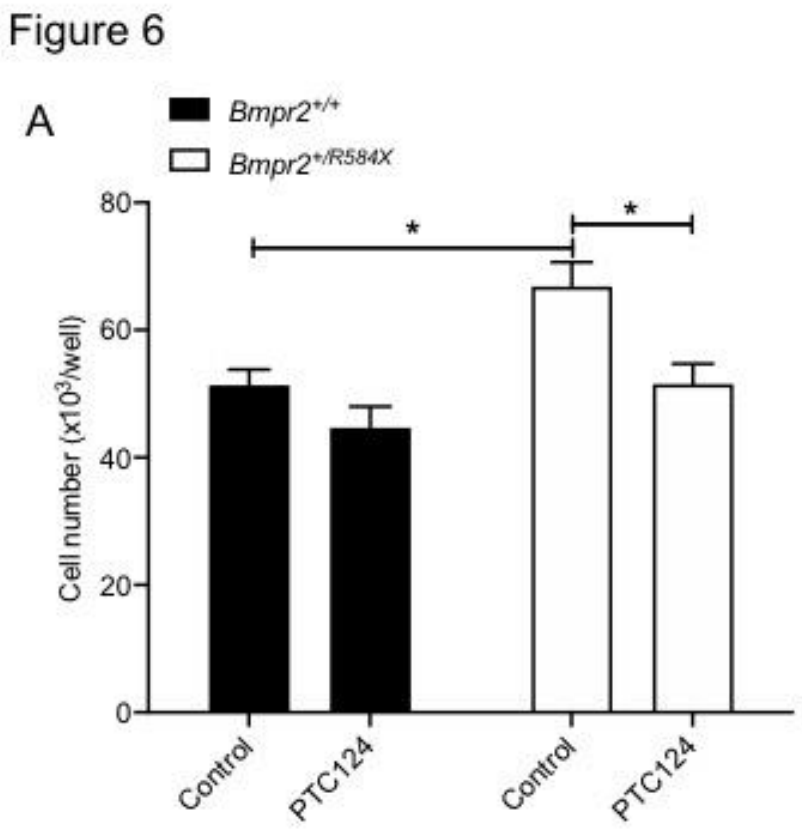

Figure 6. *Bmpr2*$^{+/R584X}$ PASMCs hyperproliferation is rescued by PTC124 treatment. Mouse PASMCs were isolated from lungs of wild-type or R584X mutant animals. Proliferation assessment of *Bmpr2*$^{+/+}$ (n=3) and *Bmpr2*$^{+/R584X}$ (n=3) PASMCs after day 6, following PTC124 (100 µM) treatment. One-way ANOVA. *P≤0.05. Error bars represent mean ± s.e.m.

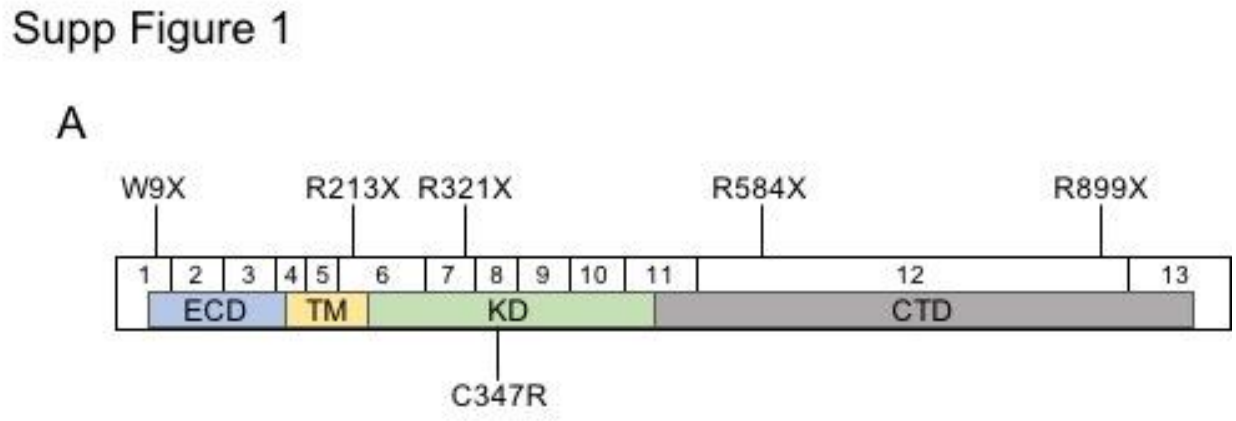

Supplementary Figure 1. BMPR2 schematic detailing the locations of the mutants used in the study. ECD – extracellular domain; TM – transmembrane; KD – kinase domain; CTD – cytoplasmic domain.

DOI: 10.1177/2045894020935783

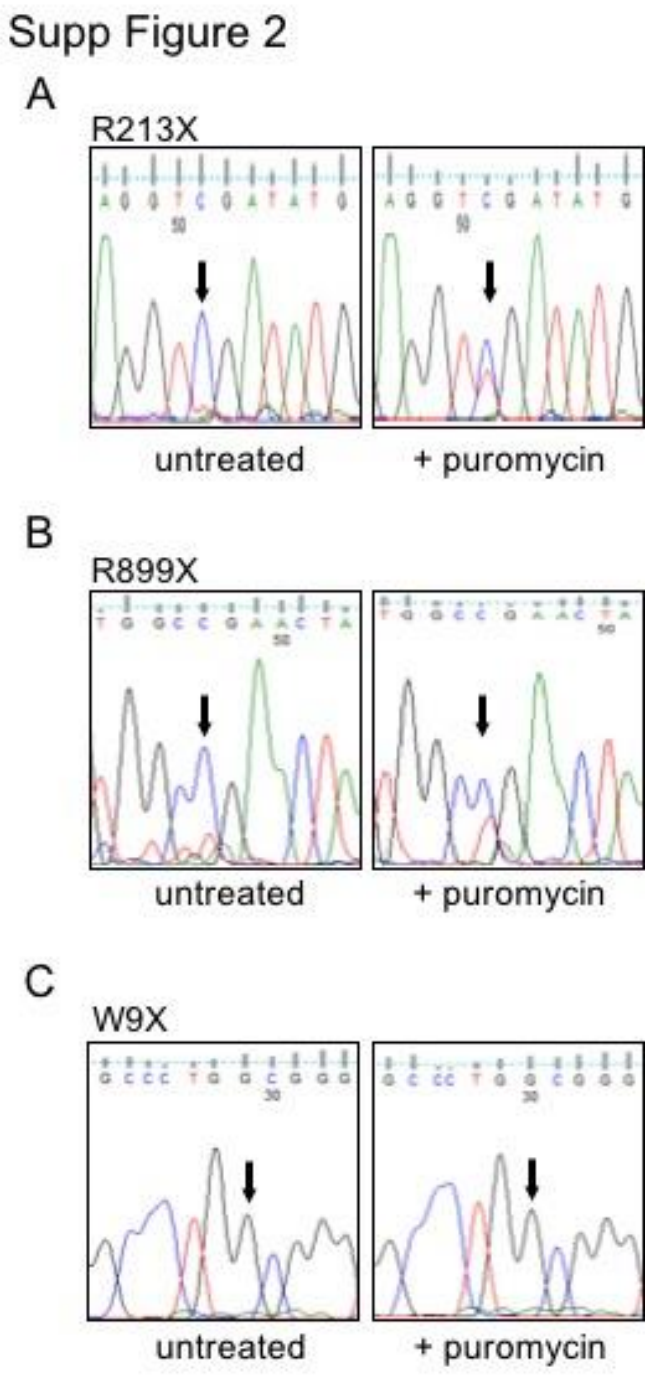

Supplementary Figure 2. Suppression of NMD using puromycin in BMPR2 mutant BOECs. (**A**, **B** and **C**) BOECs harbouring a R213X, R899X or W9X were treated overnight with puromycin (100 mg/ml). Following RNA isolation amplified RT-PCR products were sequenced. Chromatograms for R213X (**A**), R899X (**B**) and W9X (**C**) show the effects of puromycin treatment on transcript expression.

DOI: 10.1177/2045894020935783

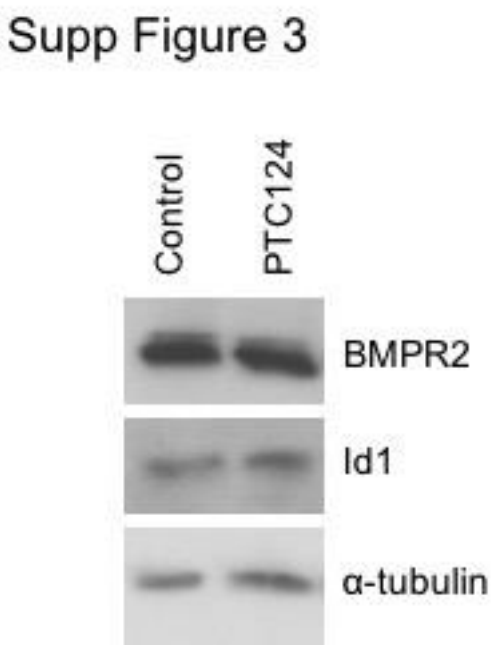

Supplementary Figure 3. PTC124 treatment does not increase BMPR2 protein expression and downstream signalling in control BOECs. BOECs isolated from control subjects were treated with PTC124 (100 μM) for 24 hours. Lysates were immunoblotted for BMPR2, Id1 and loading control, α-tubulin.

DOI: 10.1177/2045894020935783

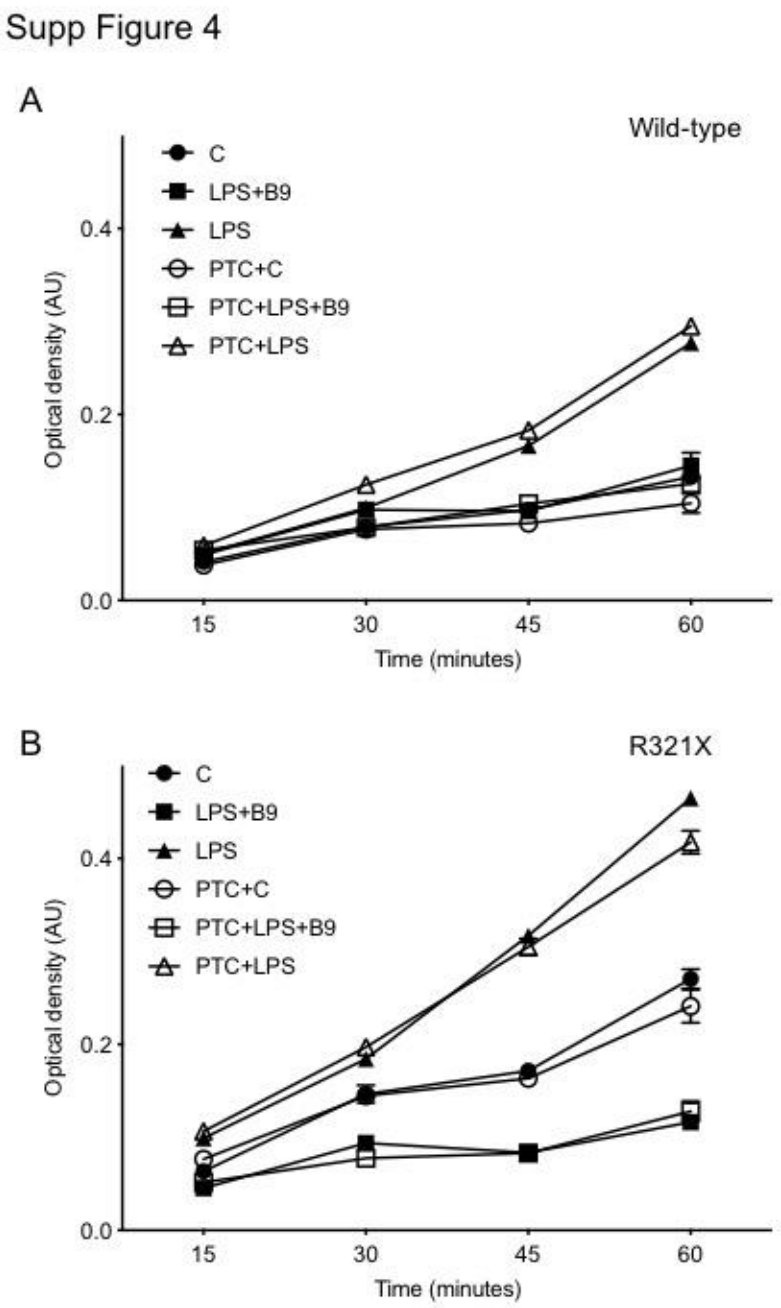

Supplementary Figure 4. Monolayer integrity in R312X mutant BOECs following PTC124 treatment. Permeability was assessed in monolayers of wild-type (**A**) (n=3) and R321X mutant (**B**) (n=3) BOECs treated with either PTC124 (100 μM) or BMP9 (0.2 ng/ml) and/or LPS (400 ng/ml). Colorimetric absorbance of HRP was measured after incubation periods every 15 minutes until 1 hour.

DOI: 10.1177/2045894020935783

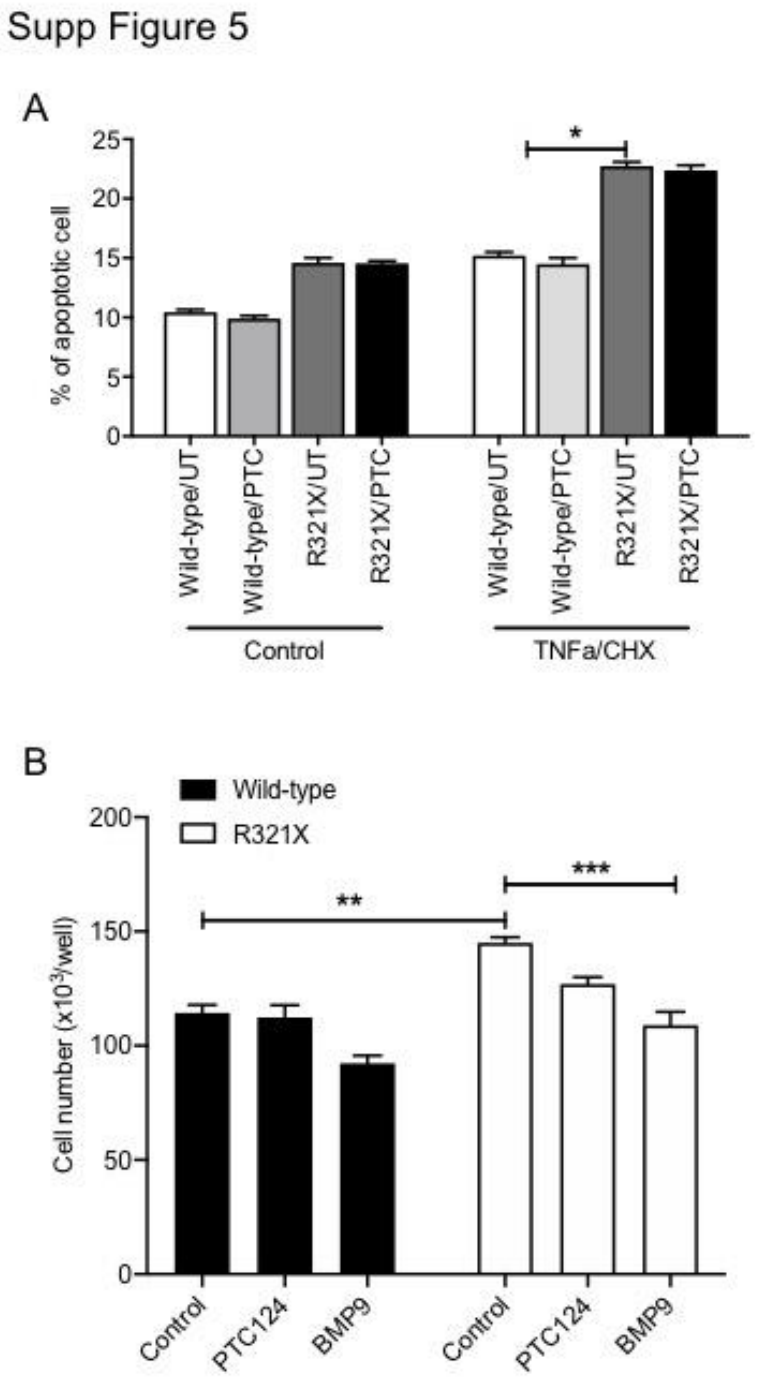

Supplementary Figure 5. Apoptosis and hyperproliferation assessment in R321X mutant BOECs. (**A**) Quantification of apoptotic (Annexin-V^+/PI^-) wild-type and R321X mutant BOECs after PTC124 treatment for 24 hours prior to the addition of TNFa (10 ng/ml) and cycloheximide (20 mg/ml) for 6 hours. (**B**) Proliferation assessment of wild-type and R321X mutant BOECs after day 6, following PTC124 (100 μM) or BMP9 (5 ng/ml) treatment. *P≤0.05, **P≤0.01, ***P≤0.001. Error bars represent mean ± s.e.m.

DOI: 10.1177/2045894020935783

Supp Figure 6

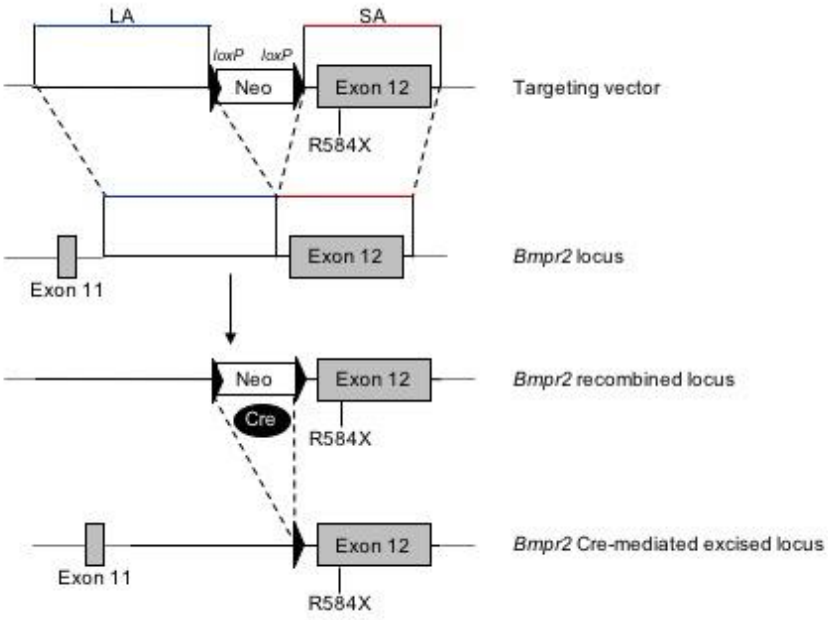

Supplementary Figure 6. Schematic of *Bmpr2*$^{+/R584X}$ mouse generation. A targeting vector containing the R584X mutation in exon 12 was generated. Upstream of the 3' short homology arm a *lox-P* flanked neomycin cassette was inserted. Chimeric males were crossed with Cre-deleter mice to excise the loxP flanked neomycin cassette.

DOI: 10.1177/2045894020935783

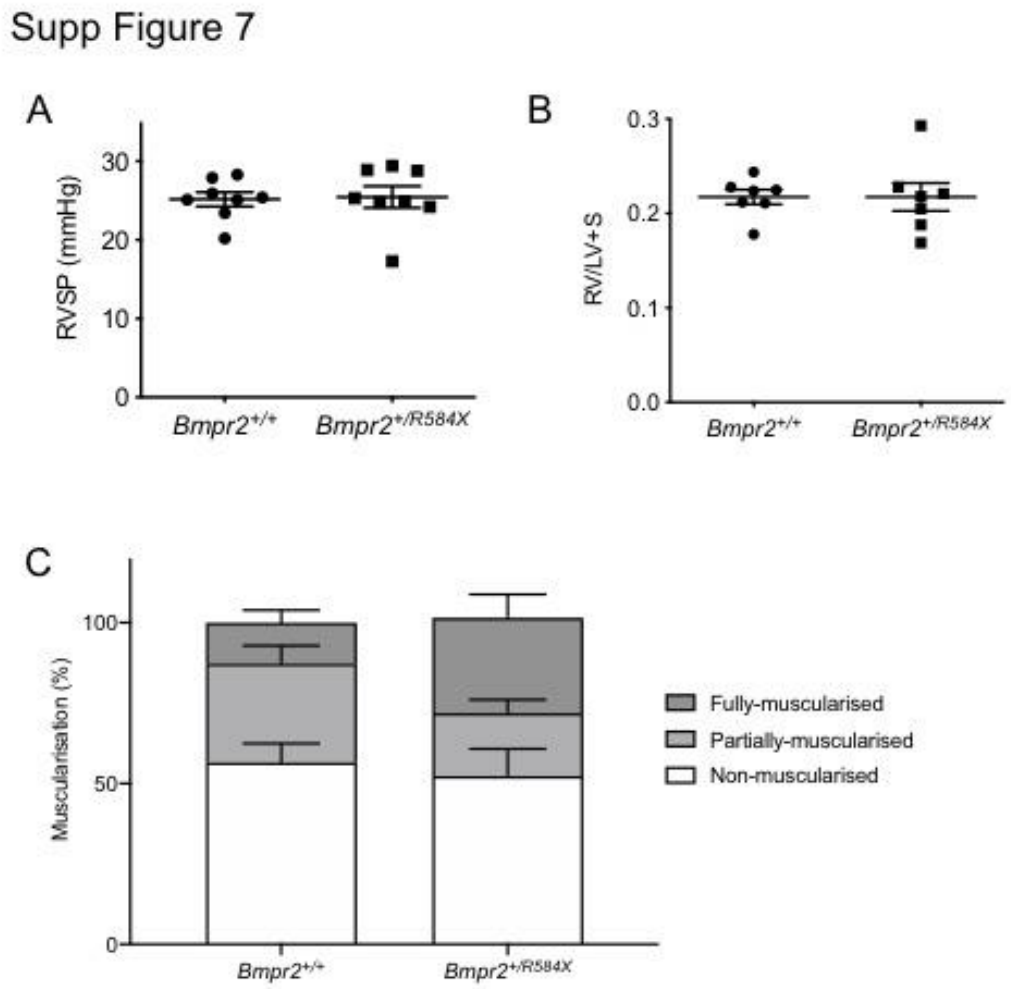

Supplementary Figure 7. Characterisation of *Bmpr2*$^{+/R584X}$mice. Assessment of right ventricular systolic pressure (RVSP) and right ventricular hypertrophy (Fulton index (RV/LV+S). (**A**) RVSP in wild-type (*Bmpr2*$^{+/+}$; n= 7) and R584X mutant (*Bmpr2*$^{+/R584X}$; n=8) mice. (**B**) Fulton index in *Bmpr2*$^{+/+}$ (n=7) and *Bmpr2*$^{+/R584X}$ (n=7) mice. Vascular remodelling quantification after PTC124 treatment. (**C**) Quantification of pulmonary artery wall thickness as a percentage of luminal area of the following groups - *Bmpr2*$^{+/+}$ +normal chow (n=); *Bmpr2*$^{+/+}$ +PTC124 chow (n=); *Bmpr2*$^{+/R584X}$ +normal chow (n=); *Bmpr2*$^{+/R584X}$ +PTC124 chow (n=). (**D**) Quantification of non, partially and fully muscularised vessels as a percentage of total alveolar and duct arteries of the following groups - *Bmpr2*$^{+/+}$ +normal chow (n=); *Bmpr2*$^{+/+}$ +PTC124 chow (n=); *Bmpr2*$^{+/R584X}$+normal chow (n=); *Bmpr2*$^{+/R584X}$ +PTC124 chow (n=). *P≤0.05. Error bars represent mean ± s.e.m.